SLC4A2-mediated Cl^-/HCO_3^- exchange activity is essential for calpain-dependent regulation of the actin cytoskeleton in osteoclasts

Fabienne Coury[a,b,c], Serhan Zenger[b,c,1], Andrew K. Stewart[d,1], Sebastien Stephens[b,c], Lynn Neff[b,c], Kelly Tsang[a], Gary E. Shull[e], Seth L. Alper[d], Roland Baron[b,c,2], and Antonios O. Aliprantis[a,b,f,2,3]

[a]Department of Immunology and Infectious Diseases, Harvard School of Public Health, Boston, MA 02115; [b]Department of Medicine, Harvard Medical School, Boston, MA 02115; [c]Department of Oral Medicine Infection and Immunity, Harvard School of Dental Medicine, Boston, MA 02115; [d]Renal Division and Molecular and Vascular Medicine Unit, Beth Israel Deaconess Medical Center, Harvard Medical School, Boston, MA 02115; [e]Department of Molecular Genetics, Biochemistry, and Microbiology, University of Cincinnati College of Medicine, Cincinnati, OH 45267; and [f]Division of Rheumatology, Department of Medicine, Brigham and Women's Hospital, Boston, MA 02115

Edited by Laurie H. Glimcher, Weill Cornell Medical College, New York, NY, and approved December 17, 2012 (received for review April 19, 2012)

Bone remodeling requires osteoclasts to generate and maintain an acidified resorption compartment between the apical membrane and the bone surface to solubilize hydroxyapatite crystals within the bone matrix. This acidification process requires (*i*) apical proton secretion by a vacuolar H^+-ATPase, (*ii*) actin cytoskeleton reorganization into a podosome belt that forms a gasket to restrict lacunar acid leakage, and (*iii*) basolateral chloride uptake and bicarbonate extrusion by an anion exchanger to provide Cl^- permissive for apical acid secretion while preventing cytoplasmic alkalinization. Here we show that osteoclast-targeted deletion in mice of solute carrier family 4 anion exchanger member 2 (*Slc4a2*) results in osteopetrosis. We further demonstrate a previously unrecognized consequence of SLC4A2 loss of function in the osteoclast: dysregulation of calpain-dependent podosome disassembly, leading to abnormal actin belt formation, cell spreading, and migration. Rescue of SLC4A2-deficient osteoclasts with functionally defined mutants of SLC4A2 indicates regulation of actin cytoskeletal reorganization by anion-exchange activity and intracellular pH, independent of SLC4A2's long N-terminal cytoplasmic domain. These data suggest that maintenance of intracellular pH in osteoclasts through anion exchange regulates the actin superstructures required for bone resorption.

Adult bone mass is determined by the rates of bone formation by osteoblasts and bone resorption by osteoclasts. An imbalance in bone remodeling favoring resorption over formation contributes to many skeletal disorders, including osteoporosis. Osteoclasts are multinucleated giant cells formed by fusion of myeloid precursors in response to the stromal factors macrophage-colony stimulating factor (M-CSF) and receptor activator for nuclear factor κB ligand (RANKL). Contact with bone matrix polarizes the osteoclast to form a sealing zone, assembled from actin-rich podosomes that mediate cell attachment and migration of motile cells (1). Podosomes consist of a core of densely packed F-actin filaments with associated proteins such as cortactin and gelsolin (1). The core is surrounded by a less dense F-actin "cloud," which colocalizes with attachment proteins such as integrins and vinculin (2, 3). In osteoclasts cultured on glass, podosomes initially group into clusters, which coalesce into rings and expand to the cell periphery to form a belt in the mature cell (4). This podosome belt is equivalent to the sealing zone formed in bone-resorbing osteoclasts in situ (3). The two structures share the same components and are stabilized by microtubules (2, 5). The sealing zone surrounds a specialized membrane domain, the ruffled border, through which hydrochloric acid and lysosomal proteases are secreted to dissolve bone mineral and digest organic matrix, respectively (6). The sealing zone serves as a gasket to anchor the osteoclast to bone and isolate the extracellular resorptive microenvironment (7, 8).

As osteoclasts secrete acid across the ruffled border (9), a base equivalent is left in the cytoplasm. To prevent cytoplasmic alkalinization, electroneutral exchange of intracellular bicarbonate for extracellular chloride occurs through anion exchange at the basolateral membrane (10). This anion exchanger was identified in our report that solute carrier family 4 anion exchanger member $2^{-/-}$ (*Slc4a2*) mice display osteopetrosis associated with dysfunctional osteoclasts (11), a finding corroborated by others (12–14). Although it is known that SLC4A2-deficient osteoclast-like cells (OCLs) are unable to resorb mineralized tissue and cannot form an acidified extracellular resorption compartment in vitro, the function of this molecule within the complex cell biology of the osteoclast remains incompletely understood. Furthermore, $Slc4a2^{-/-}$ mice display abnormalities that could indirectly affect bone metabolism, including achlorhydria, failed tooth formation, runting, and early lethality (15). These systemic abnormalities, as well as a proposed role for anion exchange in other bone cells, including osteoblasts (16, 17), require a cell-specific ablation approach to establish and characterize the osteoclast-intrinsic role in the observed skeletal phenotype.

SLC4A2 belongs to a subfamily of three homologous Na^+-independent HCO_3^-/Cl^- anion-exchanger proteins: SLC4A1/AE1 (band 3 of the red blood cell and renal type A intercalated cell), SLC4A2/AE2, and SLC4A3/AE3. Each contains a three-domain structure including an N-terminal cytoplasmic domain of 400–700 amino acids, a central anion-exchange domain that spans the membrane 12–14 times, and a short C-terminal cytoplasmic domain. In the red blood cell, the amino-terminal cytoplasmic domain of SLC4A1 tethers the membrane to the cytoskeleton. Accordingly, mutations in *SLC4A1* cause membrane instability, resulting in hereditary spherocytosis and stomatocytosis (18).

Here we demonstrate the osteoclast-intrinsic role of SLC4A2 in vivo using a conditional deletion strategy, and show that osteoclasts lacking SLC4A2 display not only altered intracellular pH (pH_i) and resorption but also spreading abnormalities associated with an enhanced life span of individual podosomes within the actin belt. Regulation of the actin cytoskeleton and bone resorption by SLC4A2 is independent of its large N-terminal cytoplasmic domain and can be ascribed solely to its anion-exchange function. SLC4A2-deficient OCLs also display a reduction in calpain protease activity, which is necessary for podosome disassembly. Moreover, cell-permeable inhibitors of

Author contributions: F.C., S.Z., A.K.S., S.L.A., R.B., and A.O.A. designed research; F.C., S.Z., A.K.S., S.S., L.N., K.T., and A.O.A. performed research; G.E.S., S.L.A., R.B., and A.O.A. contributed new reagents/analytic tools; F.C., S.Z., A.K.S., S.S., L.N., S.L.A., R.B., and A.O.A. analyzed data; and F.C., S.Z., A.K.S., S.L.A., R.B., and A.O.A. wrote the paper.

The authors declare no conflict of interest.

This article is a PNAS Direct Submission.

[1]S.Z. and A.K.S. contributed equally to this work.

[2]R.B. and A.O.A. contributed equally to this work.

[3]To whom correspondence should be addressed. E-mail: aaliprantis@partners.org.

This article contains supporting information online at www.pnas.org/lookup/suppl/doi:10.1073/pnas.1206392110/-/DCSupplemental.

calpain reproduce the spreading defect and enhanced podosome life span seen in OCLs lacking SLC4A2.

Results

Establishment of the Osteoclast-Intrinsic Role of SLC4A2. To establish the osteoclast-specific role of SLC4A2, we crossed mice bearing an *Slc4a2* allele flanked by loxP sites with cathepsin K-Cre (*Ctsk-Cre*) transgenic mice (19). In contrast to mice germ line-deficient in all *Slc4a2* isoforms (15), *Slc4a2*$^{fl/fl}$ *Ctsk-Cre*$^{+}$ mice (referred to hereafter as cKO mice) did not exhibit early lethality or growth retardation, and were not edentulous (Fig. 1*A*). Microcomputed tomography analysis showed clubbing of the long bones with decreased marrow space (Fig. 1*B*) and increased trabecular bone volume at 3 and 8 wk (Fig. 1*C*). This increased bone volume was largely secondary to increased trabecular number and, to a lesser extent, increased trabecular thickness, whereas trabecular spacing was reduced (Fig. S1*A*). The trabecular bone in the metaphysis of cKO mice contained cartilage remnants from the growth plate, a pathologic feature of osteopetrosis, as evidenced by dark purple staining with toluidine blue (Fig. 1*D*). Tartrate-resistant acid phosphatase (TRAP) staining showed increased osteoclast number in cKO tibiae compared with control (Fig. 1*E*). These data indicate that SLC4A2 plays a critical, cell-intrinsic role in mouse osteoclast function in vivo.

Conditional Deletion of *Slc4a2*^{fl} with *Ctsk-Cre* Is Incomplete in Vitro, Resulting in Partially Reduced Osteoclast Function. *Slc4a2*$^{-/-}$ OCLs are defective in cell spreading and bone resorption in vitro (11). In contrast, cKO OCLs formed resorption pits on bone slices (Fig. 1*F*), but their activity was quantitatively reduced (Fig. 1*G*), although the number of OCLs was similar to controls (Fig. S1*B*). cKO OCLs also displayed a partial decrease in spread OCLs (Fig. 1*H*). Consistent with these incomplete phenotypes, the expression of *Slc4a2* mRNA in cKO OCLs was reduced by only 70% compared with wild-type (WT) levels (Fig. S1*C*). Because only partial deletion of *Slc4a2*^{fl} was achieved in vitro using *Ctsk-Cre*, cells with either a germ-line mutation or complete inducible deletion of *Slc4a2*^{fl} using *Mx1-Cre* were used for subsequent studies.

SLC4A2 Regulates Cell Spreading and Actin Cytoskeletal Organization in Osteoclasts. TRAP-stained SLC4A2-deficient OCLs fail to spread normally in vitro (11) (Fig. 1*H*). *Slc4a2*$^{-/-}$ OCLs stained for actin displayed a pericellular belt with a significantly reduced diameter (Fig. 2*A*), confirming the spreading defect. Consistent with this cytoskeletal defect, SLC4A2-deficient OCLs showed slower migration rates compared with WT (Fig. 2*B*). The abnormal morphology of SLC4A2-deficient osteoclasts was confirmed in vivo. Compared with WT, *Slc4a2*$^{-/-}$ osteoclasts exhibited smaller ruffled borders that did not extend deep into the cytoplasm (Fig. 2*C*). Immunofluorescence revealed that SLC4A2-deficient osteoclasts often formed several small (Fig. S2*A*) but dense actin patches (Fig. 2*D*) resembling sealing zones. Consistent with the failure to form a ruffled border, the V-ATPase was not targeted to the apical membrane between the sealing zones in SLC4A2-deficient osteoclasts (Fig. 2*D*). Based on these results, we hypothesized that SLC4A2 regulates the osteoclast cytoskeleton. To explore this, we examined the organization of podosomes in *Slc4a2*$^{+/+}$ and *Slc4a2*$^{-/-}$ OCLs as defined in Fig. 3*A*. During the course of differentiation, more SLC4A2-deficient OCLs displayed actin clusters and fewer progressed to develop rings or a mature actin belt (Fig. 3*B*), suggesting that SLC4A2 regulates the dynamic organization of podosomes. Furthermore, the thicker actin belts of *Slc4a2*$^{-/-}$ OCLs consisted of uniformly enlarged, punctate podosomes (Fig. 3 *C* and *D*). The width of the sealing zone, the functional equivalent of the actin belt when OCLs are cultured on a resorptive surface, was also thicker in *Slc4a2*$^{-/-}$ OCLs (Fig. 3*E*). Podosomes in *Slc4a2*$^{-/-}$ OCLs still exhibited the typical organization of an actin core surrounded by the adhesion molecule vinculin, which colocalized with the actin cloud (Fig. S2*B*). Tubulin, which stabilizes the organization of actin, was also distributed similarly (Fig. S2*C*). Last, we previously reported reduced differentiation of *Slc4a2*$^{-/-}$ OCLs (11), which could indirectly affect spreading. However, under the culture

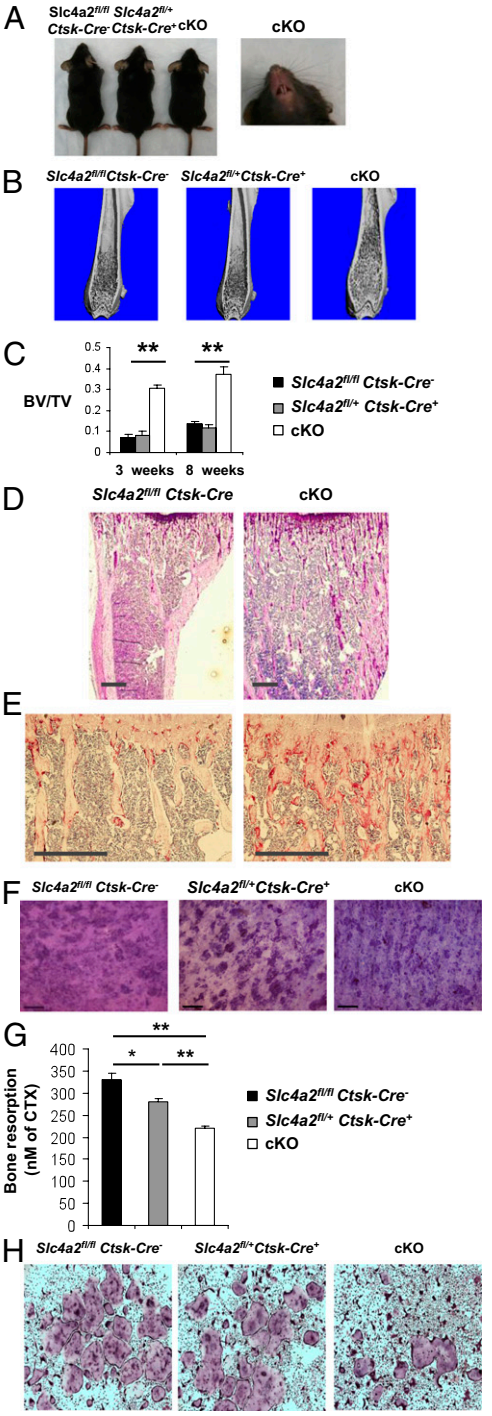

Fig. 1. Osteoclast-intrinsic role of SLC4A2. (*A*) Photographs of 3-wk-old mice. (*B*) Three-dimensional microquantitative computed tomography images of femurs from 8-wk-old mice. (*C*) Bone volume per tissue volume (BV/TV) (means ± SE) of the distal femoral metaphysis of 3- and 8-wk-old mice (**$P < 0.01$, cKO versus *Slc4a2*$^{fl/fl}$ *Ctsk-Cre*$^{-}$; similar results were obtained when cKO was compared with *Slc4a2*$^{fl/+}$ *Ctsk-Cre*$^{+}$). (*D* and *E*) Toluidine blue (*D*) and TRAP (*E*) stains of tibiae from 8-wk-old mice. Images are representative of at least three sex- and age-matched littermate mice analyzed per genotype. (Scale bars, 500 μm.) (*F* and *G*) Toluidine blue stain (*F*) and supernatant C-terminal type I collagen fragments (CTX) ELISA (*G*) (means ± SE) of bone slices incubated with bone marrow macrophages and M-CSF and RANKL. (Scale bars, 200 μm.) Representative of three separate experiments (*$P < 0.05$, **$P < 0.01$). (*H*) TRAP stain of OCLs.

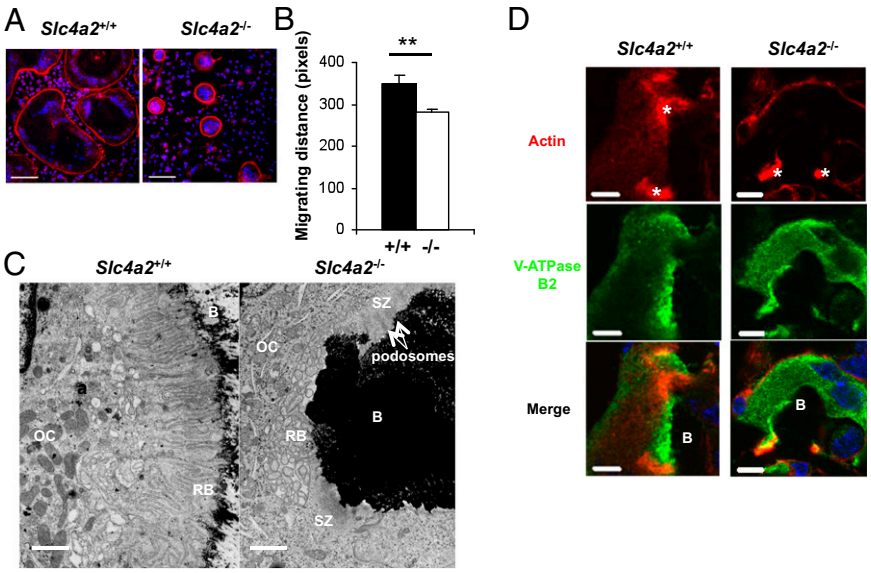

Fig. 2. Abnormal morphology and migration of *Slc4a2*$^{-/-}$ osteoclasts. (*A*) Confocal images of F-actin (red) and nuclei (blue) in OCLs. (Scale bars, 100 μm.) (*B*) Distance moved (means ± SE) over 5 h by OCLs (**$P < 0.005$). (*C* and *D*) Transmission electron microscopy (*C*) and confocal images (*D*) of osteoclasts at the proximal tibial growth plate from 5-d-old mice. (*C*) Bone (B), ruffled border (RB), osteoclast (OC), and sealing zone (SZ). (Scale bars, 2 μm.) (*D*) F-actin (red), V-ATPase B2 subunit (green), nuclei (blue), and sealing zones (asterisks). (Scale bars, 5 μm.)

conditions reported here, no differences were observed in the number of OCLs with more than two nuclei (Fig. S2*D*).

Enhanced Podosome Life Span in the Actin Belts of *Slc4a2*$^{-/-}$ OCLs. To study the dynamic properties of podosomes in WT and *Slc4a2*$^{-/-}$ OCLs in real time, cells were microinjected with cDNA encoding GFP-actin. As previously visualized by phalloidin staining (Fig. 3*C*), the actin belts in live *Slc4a2*$^{-/-}$ OCLs were thicker and individual podosomes were larger and more uniformly distributed (Fig. 3*F*). GFP-actin recovery after photobleaching did not differ within podosomes of *Slc4a2*$^{+/+}$ *and Slc4a2*$^{-/-}$ OCLs (Fig. 3*G*). However, whereas average podosome life span within clusters was similar in *Slc4a2*$^{+/+}$ and *Slc4a2*$^{-/-}$ OCLs, podosome life span in belts was substantially longer in SLC4A2-deficient OCLs (Fig. 3 *H* and *I*). Thus, SLC4A2 accelerates podosome belt formation and promotes turnover of individual podosomes within the actin belt.

SLC4A2 Anion-Exchange Activity Is Required for pH_i Regulation and OCL Spreading. Anion-exchange activity and pH_i were investigated in single OCLs. When WT cells were superfused with an

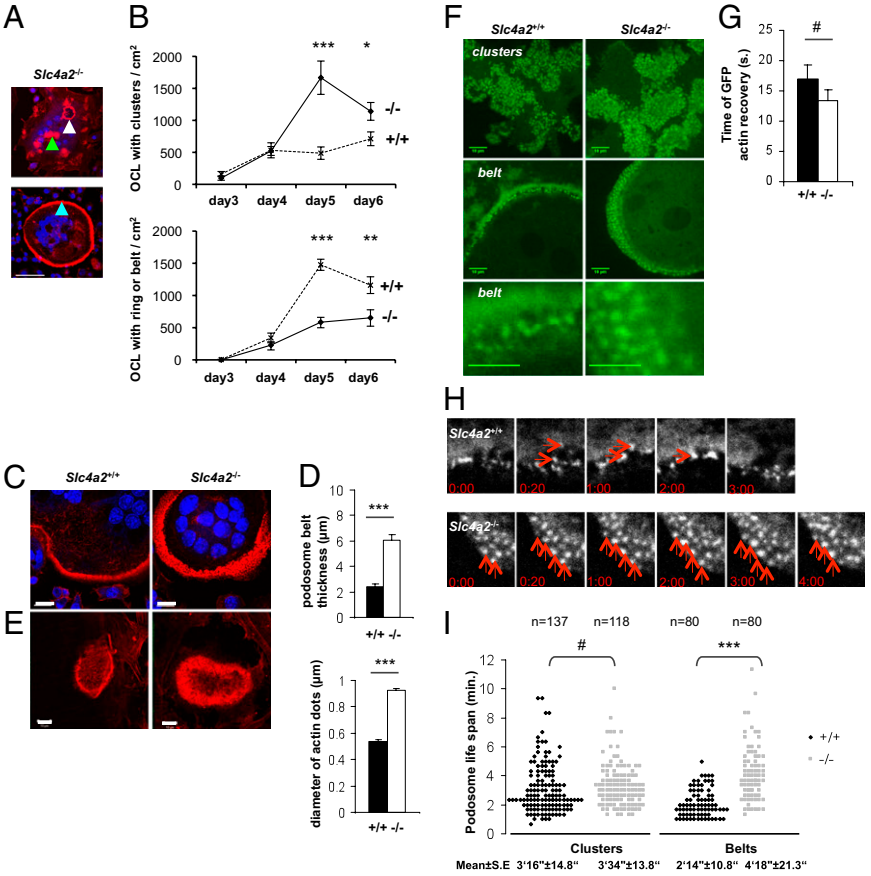

Fig. 3. Altered actin cytoskeletal dynamics in *Slc4a2*$^{-/-}$ OCLs. (*A*) Confocal images of F-actin (red) and nuclei (blue) in OCLs. Arrowheads indicate a podosome cluster (green), actin ring (white), and actin belt (blue). (Scale bar, 50 microns.) (*B*) Quantification of OCLs (>2 nuclei) per cm^2 with clusters, rings, or belts of podosomes (means ± SE) ($n = 12$; *$P < 0.01$, **$P < 0.05$, ***$P < 0.001$). (*C*) Confocal images of F-actin (red) and nuclei (blue) in OCLs. (Scale bars, 10 μm.) (*D*) Quantification of podosome belt thickness and actin dot diameter (means ± SE) in actin belts of OCLs ($n = 10$; ***$P < 0.001$). (*E*) Confocal images of F-actin (red) in OCLs plated on dentin to visualize sealing zones. (Scale bars, 10 μm.) (*F*) Images of OCLs expressing GFP-actin after microinjection. [Scale bars, 10 μm and 5 μm (unmarked).] (*G*) Fluorescence recovery after photobleaching in podosome clusters of OCLs expressing GFP-actin. Time of recovery refers to the inverse of the constant k2 [1/k2 in the equation $I(t) = I(0) - k1e^{-k2t}$] used to fit the curve of fluorescence recovery. Data are means ± SE of time of recovery from podosomes measured in three independent experiments [#n.s. (nonsignificant)]. (*H*) Time-series images extracted from observations of GFP-actin in actin belts of OCLs. Red arrows indicate individual podosomes. (*I*) Distribution of podosome life span in podosome clusters and belts of OCLs expressing GFP-actin (#n.s., ***$P < 0.001$).

HCO_3^--containing solution, followed by removal of bath Cl^- in the continued presence of CO_2/HCO_3^-, a rapid cytoplasmic alkalinization was observed (Fig. 4*A*). Restoration of extracellular Cl^- rapidly restored the original pH_i. In contrast, bath Cl^- removal did not change the pH_i in *Slc4a2*$^{-/-}$ OCLs (Fig. 4*A*). In addition, resting pH_i in *Slc4a2*$^{-/-}$ OCLs was more alkaline than in WT OCLs (Fig. 4*B*). Consistent with defective acidification of the lacunar compartment in situ (11), acidification of intracellular lysosomes in *Slc4a2*$^{-/-}$ OCLs was also largely abrogated (Fig. S3).

To determine how SLC4A2 regulates spreading, bone resorption, anion exchange, and pH_i, *Slc4a2*$^{-/-}$ OCLs were transduced with a series of functionally characterized SLC4A2 mutants (20–22) (Fig. S4*A*). These included (*i*) full-length SLC4A2a (SLC4A2-WT), (*ii*) Δ659, a deletion mutant lacking the first 659 amino acids of the N-terminal cytoplasmic domain (21), (*iii*) RL1, a chimeric protein with the pH-sensitive, putative first re-entrant loop (RL1) of the SLC4A2 transmembrane domain replaced by the corresponding pH-insensitive region of SLC4A1 (22), and (*iv*) R1056A, a missense mutant that abrogates anion-exchange activity (20). As expected, SLC4A2-WT restored anion exchange, spreading, and resorption in *Slc4a2*$^{-/-}$ OCLs (Fig. 4 *C–E* and Fig. S4*B*). Similarly, Δ659 and RL1 restored each of these functions (Fig. 4 *C–E*). In contrast, R1056A was unable to restore anion-exchange activity (Fig. 4*C*) and complemented neither the defect in resorption nor the defect in spreading observed in *Slc4a2*$^{-/-}$ OCLs (Fig. 4 *C–E* and Fig. S4*B*) despite the fact that this mutant appropriately localized to the OCL basolateral membrane (Fig. S4*C*). In addition, whereas SLC4A2-WT, Δ659, and RL1 reduced the resting pH_i in *Slc4a2*$^{-/-}$ OCLs to normal values, R1056A-expressing OCLs continued to exhibit an alkaline pH_i (Fig. 4*F*). Consistent with these results, cKO OCLs that partially maintain the ability to spread and resorb bone in vitro (Fig. 1 *G* and *H*) also displayed preserved anion-exchange activity (Fig. S4*D*), consistent with incomplete deletion of the floxed allele (Fig. S1*C*). Thus, SLC4A2 regulates bone resorption and actin cytoskeleton organization in osteoclasts via the anion exchange-dependent maintenance of pH_i.

Reduced Calpain Activity in SLC4A2-Deficient OCLs. We then hypothesized that the link between pH_i and the cytoskeleton could be via a pH-sensitive regulator of actin turnover. Calpains are pH-sensitive cysteine proteases (23), which regulate a variety of signaling cascades, including those involved in cell motility. Reduced calpain activity could therefore underlie the cytoskeletal defects observed in *Slc4a2*$^{-/-}$ osteoclasts. This hypothesis was based on the following observations. First, both μ-calpain (CAPN1) and m-calpain (CAPN2) are expressed in osteoclasts, where they localize to the actin belt (24). Second, both *Capn1*$^{-/-}$ OCLs and OCLs treated with calpain inhibitors display reduced motility and resorptive activity (24). Third, calpain inhibition in dendritic cells impairs motility and enlarges podosomes due to reduction in Wiskott–Aldrich syndrome protein (WASP) cleavage, which promotes podosome disassembly (25, 26). To generate sufficient numbers of SLC4A2-deficient OCLs for biochemical studies of calpain activity, *Slc4a2*$^{fl/fl}$ mice were crossed with *Mx1-Cre*, which can be induced postnatally by polyI:C and deletes broadly, including within the hematopoietic system (27, 28). As expected, and similar to *Slc4a2*$^{-/-}$ mice (11), *Slc4a2*$^{fl/fl}$ *Mx1-Cre* mice treated with polyI:C (hereafter *Slc4a2*$^{\Delta/\Delta}$) developed increased bone mass associated with enlarged osteoclasts that poorly attached to

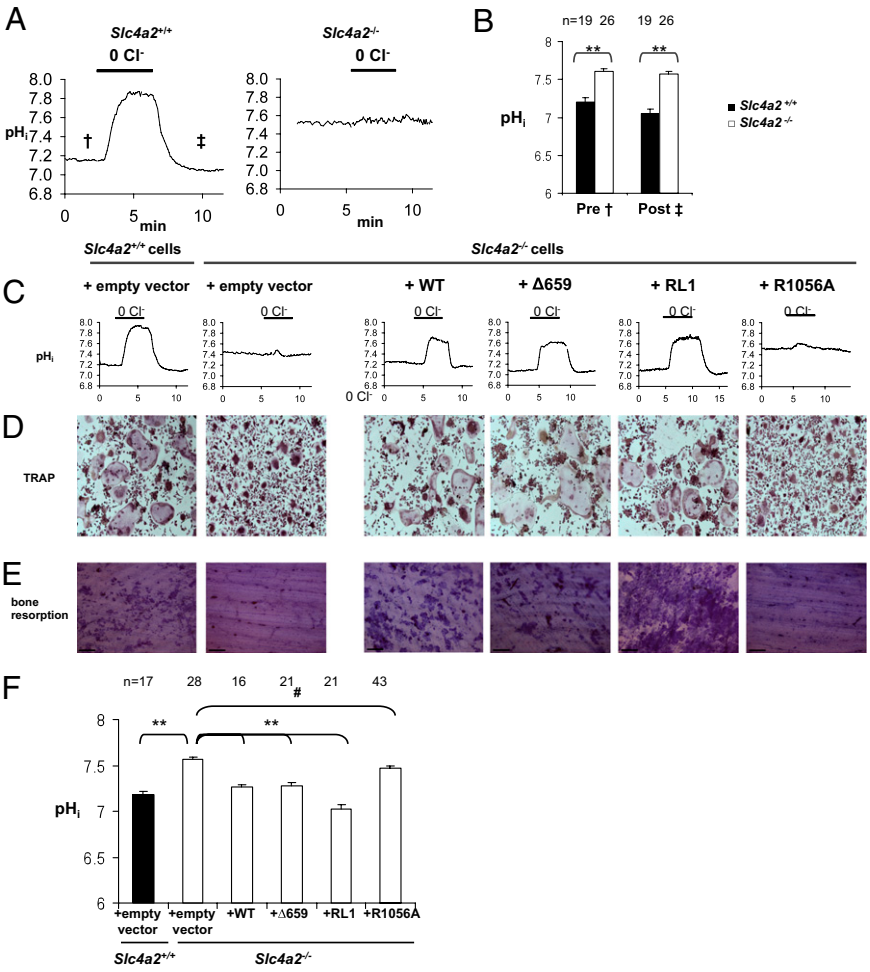

Fig. 4. Osteoclast spreading and bone resorption are dependent on SLC4A2-mediated anion exchange and regulation of pH_i. (*A*) Representative pH_i traces measured in OCLs after extracellular Cl^- removal and restoration at pH 7.4. † and ‡ indicate periods before and after Cl^- removal, respectively. (*B*) Resting pH_i in OCLs (means ± SE) measured pre- and post-Cl^- removal (**$P < 0.01$). (*C*) pH_i traces during bath Cl^- removal and restoration at pH 7.4 of OCLs transduced with the indicated SLC4A2 variants. (*D*) TRAP-stained cultures of OCLs transduced with the indicated SLC4A2 variants. (*E*) Toluidine blue-stained bone slices on which had been cultured OCLs transduced with the indicated SLC4A2 variants. Images in *D* and *E* are representative of at least three separate experiments, each performed in duplicate. (*F*) Resting post-Cl^- restoration pH_i (means ± SE) in transduced OCLs ($^{\#}$n.s., **$P < 0.01$). Resting pH_i was measured both before and after bath Cl^- removal. However, the initial resting pH_i was less stable in some cells before bath Cl^- removal, and thus post-Cl^- restoration pH_i values are reported.

bone surfaces (Fig. S5 *A–D*). In vitro, *Slc4a2*$^{\Delta/\Delta}$ OCLs did not spread normally and had undetectable levels of *Slc4a2* mRNA (Fig. S5 *E* and *F*). Despite normal levels of μ- and m-calpain protein, *Slc4a2*$^{\Delta/\Delta}$ OCLs displayed reduced calpain activity measured either by immunoblot for calpain-specific cleavage products of Rous sarcoma oncogene (SRC) and WASP or by a fluorogenic assay with a synthetic cell-permeable substrate (Fig. 5 *A–D*). Similar to SLC4A2-deficient OCLs, treatment of WT OCLs with a calpain inhibitor blocked spreading, increased the percentage of cells with podosome clusters versus belts, and augmented podosome life span (Fig. 5 *E–G*). Thus, the cytoskeletal defects observed in osteoclasts lacking SLC4A2 can be explained, at least in part, by a reduction in calpain activity.

Discussion

Of the five murine *Slc4a2* gene products, the longest, *Slc4a2a*, predominates in osteoclasts (11). *Slc4a2*$^{-/-}$ mice lack all five isoforms and display a perinatal-lethal phenotype with severe osteopetrosis (11, 13, 15). This phenotype contrasts with the milder phenotype of the *Slc4a2a,b*$^{-/-}$ mouse, in which only the *a*, *b1*, and *b2* isoforms are deleted. Although *Slc4a2a,b*$^{-/-}$ mice display augmented bone mass, the increase is mostly in cortical bone, and the mice lack the hallmark of osteopetrosis: increased trabecular bone near the growth plate (12). The milder phenotype of *Slc4a2a,b*$^{-/-}$ mice could reflect compensatory expression of SLC4A2c, differences in genetic background, or discrepant functions for SLC4A2 isoforms in other skeletal cells or tissues with hormonal and metabolic effects on bone. Supporting this last possibility are observations that SLC4A2 is expressed and functional in osteoblasts, ameloblasts, and the gut and kidney (15–17, 29). Taken together, these studies left uncertain the relative role of SLC4A2 within the osteoclast for its potential broader function in other cells involved in bone homeostasis.

Here we confirm that both osteoclast-specific and postnatal deletion of *Slc4a2*, using *Ctsk-Cre* and *Mx1-Cre*, respectively, results in osteoclast-rich osteopetrosis. The phenotype of the cKO mice generated using *Ctsk-Cre* is milder than that of germ-line deletion (11), in that the former do not display growth retardation or early lethality, and are not edentulous. This milder skeletal phenotype may reflect incomplete in vivo deletion of the *Slc4a2*^{fl} allele or a function for SLC4A2 in other bone cells. The classic osteopetrotic findings in cKO mice contrast with the milder skeletal phenotype of *Slc4a2a,b*$^{-/-}$ mice, restricted largely to increased cortical bone. Because the skeletal phenotype of cKO mice phenocopies neither the *Slc4a2*$^{-/-}$ nor *Slc4a2a,b*$^{-/-}$ mice, a function for this gene in other skeletal cells remains possible. Thus, the defects observed in *Slc4a2*$^{-/-}$ mice can be attributed to the function of this gene in osteoclasts as well as in other tissues.

Mature osteoclasts alternate between phases of migration along and attachment to the bone surface, creating successive resorption lacunae. This process depends on cell polarization and cytoskeletal rearrangements (30). The high-bone mass phenotype of mice deficient in β3-integrin, PYK2, or SRC highlights the importance of this step in bone resorption (31–33). Osteoclasts attach to bone through actin-rich podosomes, which cluster around the cell periphery to form the sealing zone (1). Here we demonstrate that SLC4A2-deficient OCLs form small, dense sealing zones in vivo and attach poorly to the bone surface. In vitro, SLC4A2-deficient osteoclasts display a delay in formation of the actin ring, the functional equivalent of the sealing zone. Once formed in these cells, however, this podosome belt is thickened and made up of enlarged podosomes with an increased life span. Because the N-terminal cytoplasmic domain of SLC4A1 anchors the red blood cell membrane to the cytoskeleton (18, 34), we hypothesized that SLC4A2 might similarly directly interact with cytoskeletal components. However, our complementation experiments demonstrate that SLC4A2 regulates the actin cytoskeleton independent of its intracellular domain and by regulating pH_i in an anion exchange-dependent manner. As the distribution of proteins that support podosome structure and the rate of actin flux within the podosomes were normal in SLC4A2-deficient osteoclasts, our data suggest that disassembly of F-actin is retarded by elevated pH_i.

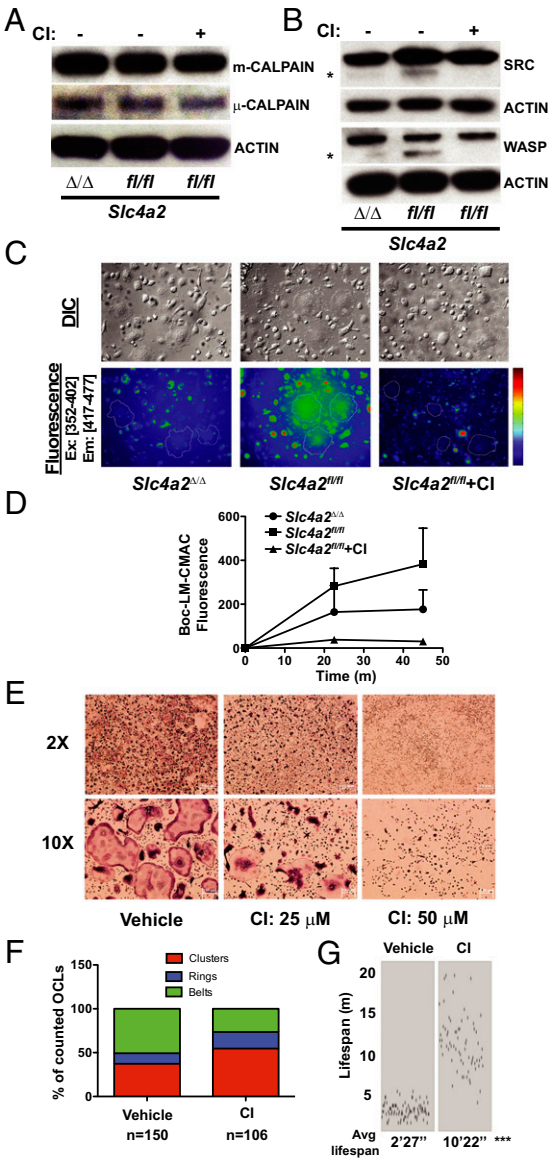

Fig. 5. Reduced calpain activity in SLC4A2-deficient OCLs. (*A* and *B*) Immunoblots of cell lysates from mature *Slc4a2*$^{fl/fl}$ and *Slc4a2*$^{\Delta/\Delta}$ OCLs. Actin was used as a loading control. Lysates from OCLs treated with calpain inhibitor (CI) MDL-28170 were used to identify calpain cleavage fragments (asterisks) of SRC and WASP. (*C* and *D*) Fluorescence image (*C*) and time-course quantification (*D*) of calpain activity in *Slc4a2*$^{fl/fl}$ and *Slc4a2*$^{\Delta/\Delta}$ OCLs in the absence or presence (*Slc4a2*$^{fl/fl}$ only) of a CI measured with a fluorogenic membrane-permeable calpain substrate t-butoxycarbonyl-Leu-Met-chloromethylaminocoumarin (Boc-LM-CMAC). (*E*) TRAP stain of WT OCLs incubated either with DMSO as vehicle or CI for 24 h. DIC, differential interference contrast microscopy. (Scale bars, 1 mm and 150 μm for 2× and 10× images, respectively.) (*F*) Quantitation of WT OCLs with actin clusters, rings, or belts after a 24-h incubation with 25 μM CI. (*G*) Life span of individual podosomes in CI-treated OCLs (***$P < 0.001$).

We found that calpain activity is reduced in osteoclasts lacking SLC4A2. Moreover, a cell-permeable calpain inhibitor recapitulates many of the features observed in SLC4A2-deficient osteoclasts, including reduced spreading and belt formation and increased podosome life span. These data support recent findings that podosome disassembly and motility in dendritic cells are promoted by calpain-mediated cleavage of WASP (25, 26). Calpain activity can be

reduced at pH above 7.5 (23, 35), but direct inhibition of calpain by elevated pH_i remains to be demonstrated. The regulation of calpain activity within cells is complex and involves autolysis and calcium-, phospholipid-, and calpastatin-mediated pathways (36), any of which could be pH_i-sensitive. Further work is needed to define how elevated pH_i reduces calpain activity in osteoclasts, and whether this pathway functions during normal cycles of bone resorption. Last, other proteins that regulate F-actin dynamics in motile cells may be pH-sensitive and changes in their activity may contribute to the observed cytoskeletal defects in *Slc4a2*$^{-/-}$ osteoclasts.

The ability of the Δ659 mutant to restore resting pH_i and anion-exchange function in *Slc4a2*$^{-/-}$ OCLs is concordant with previous studies demonstrating intact anion exchange in mutants lacking the majority of the SLC4A2 N-terminal cytoplasmic domain (18). However, the N-terminal cytoplasmic domain is required for acute inhibition of SLC4A2 by acidic pH (21). Similarly, RL1 of the SLC4A2 transmembrane domain is also critical for regulation by pH_i (22), but the RL1 mutant restored the abnormal phenotype of *Slc4a2*$^{-/-}$ OCLs. Our results suggest that neither acute pH sensitivity of SLC4A2 nor the SLC4A2 cytoplasmic domain is required for bone resorption by OCLs. However, within the bone microenvironment, these domains may play a regulatory role.

Our results demonstrate the osteoclast-intrinsic role of SLC4A2 in bone resorption in vivo and show that SLC4A2 mediates cytoskeletal organization in osteoclasts by regulating calpain activity via anion exchange-dependent control of pH_i.

Materials and Methods

Mice. *Slc4a2*$^{-/-}$ mice were previously described (15). The *Slc4a2*^{fl} allele was generated by flanking exon 8 with loxP sites, and will be described in detail elsewhere. Cre-mediated deletion of the 181-nt exon 8 (numbered according to Ensembl transcript variant Slc4a2-001; GenBank accession no. NM_009207.3), which is present in all *Slc4a2* variants, removes codons 319–378 and generates a frame-shift that eliminates the membrane-spanning domains needed for anion-transport activity. The *Slc4a2*^{fl} allele was deleted specifically in osteoclasts or in adolescent mice using cathepsin K-Cre [kindly provided by S. Kato (University of Tokyo, Tokyo, Japan) (19)] or *Mx1-Cre* and treating mice with polyI:C as described (27), respectively. The Standing Committee on Animals at Harvard Medical School approved all experimental protocols.

Preparation of OCLs. See *SI Materials and Methods*.

Microinjection and Time-Lapse Microscopy. See *SI Materials and Methods*.

Single-Cell Measurement of pH_i. See *SI Materials and Methods*.

Calpain Activity Assay. See *SI Materials and Methods*.

ACKNOWLEDGMENTS. We thank the Harvard Neurodiscovery Center Optical Imaging Program for assistance with microscopy. F.C. was supported by the International Bone and Mineral Society, Société Française de Rhumatologie, Association pour la Recherche sur le Cancer, and The Philippe Foundation. G.E.S. was supported by R01DK-050594 from the National Institute of Diabetes and Digestive and Kidney Diseases. S.L.A. was supported by National Institutes of Health Grant DK43449 and Harvard Digestive Diseases Center Grant DK34854. A.O.A. holds a Career Award for Medical Scientists from the Burroughs Wellcome Fund, and this work was supported by K08AR-054859 and R01AR-060363 from National Institute of Arthritis and Musculoskeletal and Skin (NIAMS) Diseases (to A.O.A.) and Grants R01AR-49879 and R01AR-054450 from NIAMS (to R.B.).

1. Linder S, Aepfelbacher M (2003) Podosomes: Adhesion hot-spots of invasive cells. *Trends Cell Biol* 13(7):376–385.
2. Destaing O, Saltel F, Géminard JC, Jurdic P, Bard F (2003) Podosomes display actin turnover and dynamic self-organization in osteoclasts expressing actin-green fluorescent protein. *Mol Biol Cell* 14(2):407–416.
3. Luxenburg C, et al. (2007) The architecture of the adhesive apparatus of cultured osteoclasts: From podosome formation to sealing zone assembly. *PLoS One* 2(1):e179.
4. Saltel F, Chabadel A, Bonnelye E, Jurdic P (2008) Actin cytoskeletal organisation in osteoclasts: A model to decipher transmigration and matrix degradation. *Eur J Cell Biol* 87(8-9):459–468.
5. Destaing O, et al. (2005) A novel Rho-mDia2-HDAC6 pathway controls podosome patterning through microtubule acetylation in osteoclasts. *J Cell Sci* 118(Pt 13): 2901–2911.
6. Rousselle AV, Heymann D (2002) Osteoclastic acidification pathways during bone resorption. *Bone* 30(4):533–540.
7. Baron R, Neff L, Louvard D, Courtoy PJ (1985) Cell-mediated extracellular acidification and bone resorption: Evidence for a low pH in resorbing lacunae and localization of a 100-kD lysosomal membrane protein at the osteoclast ruffled border. *J Cell Biol* 101(6):2210–2222.
8. Teitelbaum SL, Ross FP (2003) Genetic regulation of osteoclast development and function. *Nat Rev Genet* 4(8):638–649.
9. Blair HC, Teitelbaum SL, Ghiselli R, Gluck S (1989) Osteoclastic bone resorption by a polarized vacuolar proton pump. *Science* 245(4920):855–857.
10. Teti A, et al. (1989) Cytoplasmic pH regulation and chloride/bicarbonate exchange in avian osteoclasts. *J Clin Invest* 83(1):227–233.
11. Wu J, Glimcher LH, Aliprantis AO (2008) HCO_3^-/Cl^- anion exchanger SLC4A2 is required for proper osteoclast differentiation and function. *Proc Natl Acad Sci USA* 105(44):16934–16939.
12. Jansen ID, et al. (2009) Ae2(a,b)-deficient mice exhibit osteopetrosis of long bones but not of calvaria. *FASEB J* 23(10):3470–3481.
13. Josephsen K, et al. (2009) Targeted disruption of the Cl^-/HCO_3^- exchanger Ae2 results in osteopetrosis in mice. *Proc Natl Acad Sci USA* 106(5):1638–1641.
14. Meyers SN, et al. (2010) A deletion mutation in bovine SLC4A2 is associated with osteopetrosis in Red Angus cattle. *BMC Genomics* 11:337.
15. Gawenis LR, et al. (2004) Mice with a targeted disruption of the AE2 Cl^-/HCO_3^- exchanger are achlorhydric. *J Biol Chem* 279(29):30531–30539.
16. Lyaruu DM, et al. (2008) The anion exchanger Ae2 is required for enamel maturation in mouse teeth. *Matrix Biol* 27(2):119–127.
17. Liu L, Schlesinger PH, Slack NM, Friedman PA, Blair HC (2011) High capacity Na^+/H^+ exchange activity in mineralizing osteoblasts. *J Cell Physiol* 226(6):1702–1712.
18. Alper SL (2009) Molecular physiology and genetics of Na^+-independent SLC4 anion exchangers. *J Exp Biol* 212(Pt 11):1672–1683.
19. Nakamura T, et al. (2007) Estrogen prevents bone loss via estrogen receptor alpha and induction of Fas ligand in osteoclasts. *Cell* 130(5):811–823.
20. Stewart AK, Kurschat CE, Alper SL (2007) Role of nonconserved charged residues of the AE2 transmembrane domain in regulation of anion exchange by pH. *Pflugers Arch* 454(3):373–384.
21. Stewart AK, Kurschat CE, Vaughan-Jones RD, Shmukler BE, Alper SL (2007) Acute regulation of mouse AE2 anion exchanger requires isoform-specific amino acid residues from most of the transmembrane domain. *J Physiol* 584(Pt 1):59–73.
22. Stewart AK, Kurschat CE, Vaughan-Jones RD, Alper SL (2009) Putative re-entrant loop 1 of AE2 transmembrane domain has a major role in acute regulation of anion exchange by pH. *J Biol Chem* 284(10):6126–6139.
23. Zhao X, et al. (1998) pH dependency of mu-calpain and m-calpain activity assayed by casein zymography following traumatic brain injury in the rat. *Neurosci Lett* 247(1): 53–57.
24. Marzia M, et al. (2006) Calpain is required for normal osteoclast function and is down-regulated by calcitonin. *J Biol Chem* 281(14):9745–9754.
25. Calle Y, Carragher NO, Thrasher AJ, Jones GE (2006) Inhibition of calpain stabilises podosomes and impairs dendritic cell motility. *J Cell Sci* 119(Pt 11):2375–2385.
26. Macpherson L, et al. (2012) Tyrosine phosphorylation of WASP promotes calpain-mediated podosome disassembly. *Haematologica* 97(5):687–691.
27. Aliprantis AO, et al. (2008) NFATc1 in mice represses osteoprotegerin during osteoclastogenesis and dissociates systemic osteopenia from inflammation in cherubism. *J Clin Invest* 118(11):3775–3789.
28. Kühn R, Schwenk F, Aguet M, Rajewsky K (1995) Inducible gene targeting in mice. *Science* 269(5229):1427–1429.
29. Bronckers AL, et al. (2009) Localization and function of the anion exchanger Ae2 in developing teeth and orofacial bone in rodents. *J Exp Zoolog B Mol Dev Evol* 312B(4): 375–387.
30. Lakkakorpi PT, Väänänen HK (1996) Cytoskeletal changes in osteoclasts during the resorption cycle. *Microsc Res Tech* 33(2):171–181.
31. Gil-Henn H, et al. (2007) Defective microtubule-dependent podosome organization in osteoclasts leads to increased bone density in Pyk2(–/–) mice. *J Cell Biol* 178(6): 1053–1064.
32. McHugh KP, et al. (2000) Mice lacking beta3 integrins are osteosclerotic because of dysfunctional osteoclasts. *J Clin Invest* 105(4):433–440.
33. Soriano P, Montgomery C, Geske R, Bradley A (1991) Targeted disruption of the c-src proto-oncogene leads to osteopetrosis in mice. *Cell* 64(4):693–702.
34. Ghosh S, Cox KH, Cox JV (1999) Chicken erythroid AE1 anion exchangers associate with the cytoskeleton during recycling to the Golgi. *Mol Biol Cell* 10(2):455–469.
35. Yoshimura N, et al. (1983) Two distinct Ca^{2+} proteases (calpain I and calpain II) purified concurrently by the same method from rat kidney. *J Biol Chem* 258(14):8883–8889.
36. Goll DE, Thompson VF, Li H, Wei W, Cong J (2003) The calpain system. *Physiol Rev* 83(3):731–801.